A. STARZHYNSKA,[1] O. DMYTRENKO,[1] M. KULISH,[1] O. PAVLENKO,[1]
I. DOROSHENKO,[1] A. LESIUK,[1] T. VEKLICH,[2] M. KANIUK[2]

[1] Taras Shevchenko National University of Kyiv
(64/13, Volodymyrs"ka St., Kyiv 01601, Ukraine; e-mail: logvin-alina97@ukr.net)
[2] Institute of Biochemistry of Nat. Acad. of Sci. of Ukraine
(9, Leontovycha Str., Kyiv 01030, Ukraine)

PECULIARITIES OF THE FLUORESCENCE QUENCHING IN THE ATP – CALIX[4]ARENE C-107 AQUEOUS SOLUTIONS

UDC 539

The nature of fluorescence (FL) quenching for the aqueous solutions of adenosine triphosphate (ATP) with calix[4]arenes C-107 in the presence of silver nitrate $AgNO_3$ is studied. It is shown that, for the water solutions of ATP and calix[4]arenes C-107 at a constant concentration of ATP molecules with an increase in the content of C-107, a complex nature of the PL quenching is observed, while maintaining the position of the PL band near 395 nm (λ_{ex} = 285 nm). Its complexity is based, on the one hand, in the wide range of concentrations of C-107, at which it occurs, and, on the other hand, there are gaps in the quenching values for individual concentrations of calix[4]arene, near which it changes slightly. The indicated nature of the PL quenching significantly depends on the wavelength of excitation and the temperature. Similar quenching behavior is preserved, when $AgNO_3$ salts are added to the ATP–C-107 mixtures, ($C_{ATP} = C_{C\text{-}107} = 1 \times 10^{-4}$ M) in the concentration range from 1×10^{-4} M to 1×10^{-3} M. The computer modeling shows that the system ATP–C-107 can form energetically stable complexes, when ATP is located on the top of the calix[4]arene and along the wall of it due to π-π-stacking interaction, and the complexes are characterized by a shrinking of the energy bands.

Keywords: adenosine triphosphate, calix[4]arene C-107, fluorescence quenching, computer modeling, IR absorption.

1. Introduction

Adenosine triphosphate (ATP) belongs to one of the most important nucleotide molecules in the living organisms and performs various functions to ensure their activity [1–3]. At the same time, one of the unique functions of this molecule is the energy transfer to the cells and tissues that is released by this nucleotide during the hydrolysis of ATP, which is accompanied by dephosphorylation [1–3].

The effect of the ATP on the hydrolysis is important and can be achieved by its complexation by various receptors (ligands) accounting for the molecular structure of the nucleotide [4] A special role in these structures plays adenine, which contains nitrogen atoms capable of transferring electrons, for example, to silver cations Ag^+, creating ATP–Ag^+complexes

Citation: Starzhynska A., Dmytrenko O., Kulish M., Pavlenko O., Doroshenko I., Lesiuk A., Veklich T., Kaniuk M. Peculiarities of the fluorescence quenching in the ATP – calix[4]arene C-107 aqueous solutions. *Ukr. J. Phys.* **69**, No. 2, 71 (2024). https://doi.org/10.15407/ujpe69.2.71.
Цитування: Стражинська А., Дмитренко О., Куліш М., Павленко О., Дорошенко І., Лесюк А., Векліч Т., Канюк М. Особливості гасіння флуоресценції в розчинах у воді АТФ – калікс[4]арена С-107. *Укр. фіз. журн.* **69**, № 2, 71 (2024).

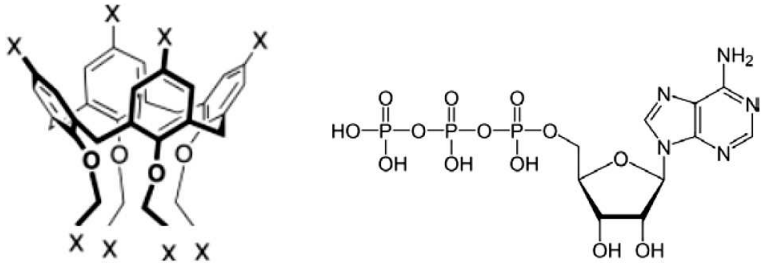

Fig. 1. Structural formula, showing four-membered model of a calixarene

due to the binding of a metal ion to N-7 or N-9 [5, 6]. Complexes of multicharged ions are more interesting, since their connection to ATP is also associated with the presence of anions in the triphosphate part of ATP [7]. In addition to the electrostatic interaction, hydrophobic, π-π stacking interactions can be formed, or hydrogen bonds can appear, that is, accompanied by the complexation of ATP with more complex molecular systems, which are often used to visualize the presence of ATP [8–11].

Such complexes are used as molecular probes, because they play an important role in biological processes. A special place among various receptors is occupied by calixarene due to its cup-like structure, see the structural formula (Fig. 1), showing four-membered model of a calixarene as an example.

Calix[4]arenes belong to macrocyclic compounds, consisting of phenolic fragments and connected by methylene bridges. The lower level of calix [4]arene includes a set of hydroxyl groups. It was shown that the supramolecular complex of the calix[4]arene receptor with the ATP substrate is formed due to the action of hydrogen bonds. Such supramolecular systems act as ATP hydrolysis catalysts, i.e. act as modulators of ATP hydrolysis structures [12].

The purpose of this work is to study the fluorescent properties of ATP in aqueous solutions with calix[4]arene C-107 and to determine the possibilities of the formation of supramolecular complexes using the PL quenching measurements and computer simulations.

2. Experimental Part

2.1. Preparation of solutions

The substance of the calix[4]arene C-107 (5,17-di(phosphono-2-pyridylmethyl)amino-11,23-di-tert-butyl-26,28-dihydroxy-25,27 dipropoxycalix[4]arene) was synthesized in the phosphorus chemistry department of the Institute of Organic Chemistry of the National Academy of Sciences of Ukraine as described in [13].

The calix[4]arene C-107 substance was dissolved in DMSO (Sigma, USA) (concentration (5%)) and, after tha, the water was added in order to obtain the concentration calix[4]arene of 1×10^{-4} M at two levels of pH 7.4 and pH 6.5. The control spectra of fluorescence (at 0 calixarene C-107) were also recorded in the presence of 5% DMSO in the solution.

The concentration of ATP molecules (Sigma Aldrich/Merck) was 1×10^{-4} M and 3×10^{-4} M. Distilled water was used with electrical conductivity not exceeding 1.5 μS/cm, pH 6.5. The electrical conductivity of water was recorded using a conductometer OK-102/1 (Hungary).

The concentration of $AgNO_3$ salt varied from $1 \times \times 10^{-4}$ M to 1×10^{-3} M at the level of pH 5.8.

In the aqueous solutions of the ATP–C-107 system, the concentration of ATP was constant ($1 \times \times 10^{-4}$ M and 3×10^{-4} M), whereas the concentrations of calix[4]arene C-107 were: 1×10^{-12}, 1×10^{-11}, 1×10^{-10}, 1×10^{-9}, 1×10^{-8}, 1×10^{-7}, 1×10^{-6}, 1×10^{-5}, 1×10^{-4} M.

The study of ATP–C-107 complexes was carried out both at constant temperatures (21 °C, 20 °C) and variable temperatures (20 °C, 30 °C, 40 °C). In the aqueous solutions of ATP–C-107–$AgNO_3$, the concentrations of ATP and C-107 were constant $C_{C\text{-}107} = = C_{ATP} = 1 \times 10^{-4}$ M. The concentrations of Ag^+ were $C_{Ag^+} = 1 \times 10^{-4}$ M, 2×10^{-4} M, 4×10^{-4} M, 6×10^{-4} M, 8×10^{-4} M, 1×10^{-3} M. Study of the ATP–C-107–$AgNO_3$ complexation was carried out at a constant temperature of 20 °C.

Optical density spectra of solutions were measured on a UV-1900 spectrophotometer (UV/Vis) (Macy, Shanghai, China). The emission and fluorescence ex-

citation spectra were measured on a spectrofluorimeter Quanta Master 40 Intensity Based Spectrofluorimeter by PTI (HORIBA Scientific, Canada).

3. Results and Discussion

3.1. Formation of ATP – calix[4]arene complexes

Hydroxyl groups of the bottom ring of the calix[4]arene C-107 form intermolecular bonds with the ATP. The presence of such bonds affects the hydrolysis of ATP in an aqueous solution in the presence of calix[4]arenes. Thus, calix[4]arene can acts as a catalyst for ATP hydrolysis reactions [14]. The reason for this intensification of hydrolysis is the formation of the complexes (calix[4]arene – ATP). It is obvious that, in the complex, first of all, the final anhydride bond P–O–P is weakened, which contributes to its break in the aqueous environment.

On the other hand, studies of the laser photolysis and pulse radiolysis indicate a weak intermolecular interaction in the ATP – calix[4]arene. At the same time, such an interaction occurs as a result of the heteroassociation of ATP with a neutral C[4] molecule with the formation of an ATP – calix[4]arene complex, which is responsible for enhancing the ATP hydrolysis.

It is assumed that the supramolecular complex ATP – calix[4]arene is formed with a neutral molecule calix[4]arene, but the association of ATP with the cation – radical calix[4]arene$^+$ upon the excitation of calix[4]arene is not excluded. For both complexation mechanisms, ATP molecules stabilize the cation – calix[4]arene$^+$ radicals, the decay of the excited state of which in complexes slows down compared to a similar decay in the absence of ATP molecules in a water solution [15].

3.2. PL quenching in water solutions of ATP and calix[4]arene

The optical absorption of ATP is described by the two peaks at 208 nm and 258 nm. At the same time, for water ATP solutions with its concentration of $1 \times \times 10^{-4}$ M, the excitation with $\lambda_{ex} = 258$ nm leads to the appearance of a low-intensity PL emission band (at pH 7.4). When the acidity increases up to pH 6.5, the PL band of the ATP solution in water at $\lambda_{ex} = = 282$ nm shifts to the red region to 395 nm.

An aqueous solution of calix[4]arene C-107 was prepared in DMSO (5%). In the absorption spectrum at pH 7.4, two bands near 272 nm and 315 nm are observed for a solution in water with a concentration of 1×10^{-4} M. When the content of C-107 is increased to 5×10^{-4} M, a strong increase in the absorption and a significant expansion of the absorption band is observed. In the case of pH 6.5 for a solution of C-107 in water with a concentration of 1×10^{-4} M at $\lambda_{ex} = 275$ nm, the PL emission band with negligible intensity and a maximum near 415 nm is formed. As the study of the PL excitation spectrum shows, the main contribution to the emission band (415 nm) is made by the absorption band near 275 nm, which has a little change compared to the maximum of the optical-density band (272 nm). The addition of C-107 solutions with different contents from 1×10^{-4} M to 1×10^{-3} M to the water solution of ATP with a constant concentration (1×10^{-4} M) leads to a complex rearrangement of the PL emission and excitation spectra at $\lambda_{ex} = 272$ nm and $\lambda_{em} = 395$ nm [16]. It should be noted that the intensity of the emission and excitation spectra of PL solutions of ATP in water greatly exceeds the intensity of similar spectra of C-107 in DMSO (5%). At the same time, the spectra depend on the excitation wavelength λ_{ex}, the pH value, and to a less extent, on the temperature in the interbal from 20 to 40 °C.

In Fig. 2, the emission and PL excitation spectra of aqueous solutions of ATP and ATP–C-107 at different concentrations of calix[4]arene and temperatures are presented.

It can be seen that, with an increase in the content of C-107, the intensity of the PL bands decreases, and the positions of the PL emission and excitation bands remain at 395 nm and 284 nm, respectively. The quenching of the PL emission with increasing the temperature from 20 °C to 40 °C increases, but varies depending on the concentration of calix[4]arene.

Figure 3 shows the PL emission and excitation spectra of ATP–C-107 solutions in water at a constant ATP concentration and with increasing the C-107 content at different temperatures.

At the same time, the induced PL quenching is observed in a wide range of concentrations from 1×10^{-9} M to 1×10^{-4} M. Moreover, there is a significant difference in the quenching values for concentrations C-107 1×10^{-9} M, 1×10^{-8} M and higher concentration values of 1×10^{-5} M, 1×10^{-4} M. The

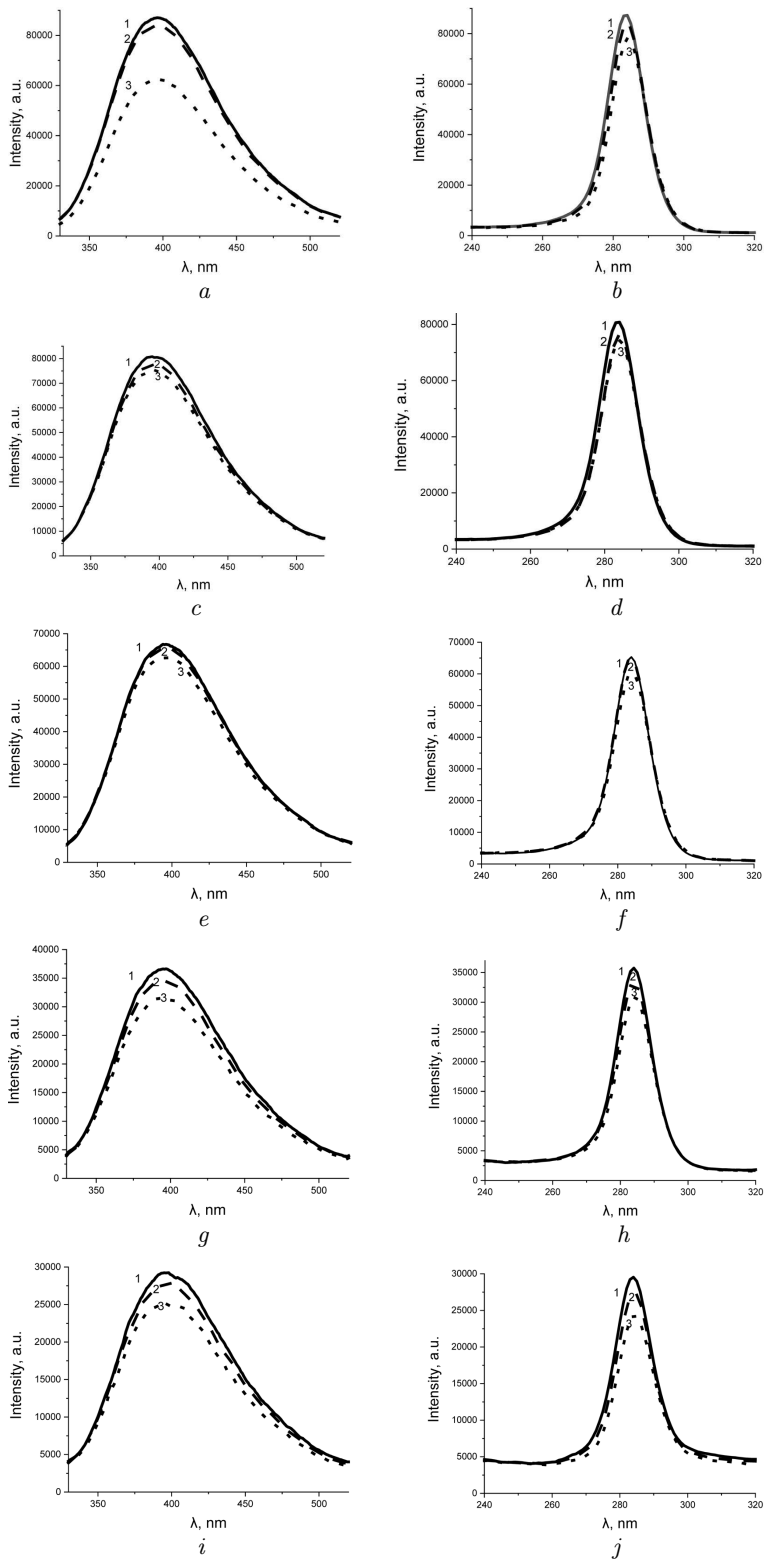

Fig. 2. Spectra of emission (*a, c, e, g, i*) and PL excitation (*b, d, f, n, j*) for solutions of ATP in water with a constant concentration of ATP $= 3 \times 10^{-4}$ M (*a, b*) and ATP–C-107 (DMSO content 0.5%) with $C_{C\text{-}107}$ concentrations of 1×10^{-9} M (*c, d*), 1×10^{-8} M (*e, f*), 1×10^{-5} M (*g, h*), 1×10^{-4} M (*i, j*) at temperatures of 20 °C (solid line *1*), 30 °C (dashed line *2*), 40 °C (dotted line *3*) ($\lambda_{ex} = 285$ nm and $\lambda_{em} = 395$ nm, pH 6.5)

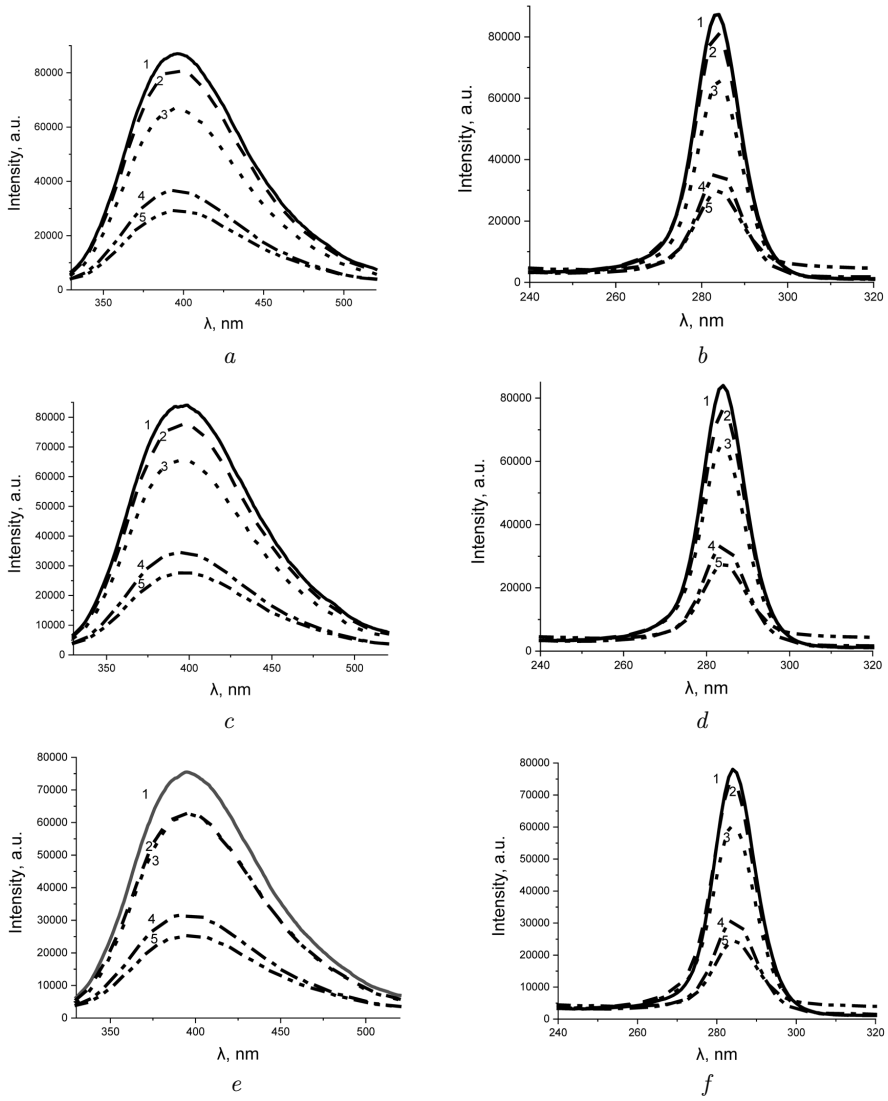

Fig. 3. Spectra of emission (*a, c, e*) and excitation (*b, d, f*) of PL for aqueous solutions of ATP–C-107 at a constant concentration of ATP $C_{ATP} = 3 \times 10^{-4}$ M and concentrations of C-107 $C_{C\text{-}107}$ 0 (solid line *1*), 1×10^{-9} M (dashed line *2*), 1×10^{-8} M (dotted line *3*), 1×10^{-5} M (dashed-dotted line *4*), 1×10^{-4} M (dashed-double dotted line *5*) at temperatures of 20 °C (*a, b*), 30 °C (*c, d*), 40 °C (*e, f*) ($\lambda_{ex} = 285$ nm and $\lambda_{em} = 395$ nm, pH 6.5)

indicated discontinuity in PL quenching is clearly visible in a wide range of C-107 concentrations for a lower ATP content.

Figure 4 shows the the PL emission and excitation spectra for aqueous solutions of ATP–C-107 in the range of calix[4]arene concentrations from 1×10^{-12} M to 1×10^{-4} M at $\lambda_{ex} = 285$ nm.

It can be seen that there are two different areas of PL quenching. The first includes ATP solutions in water with C-107 concentrations from 1×10^{-12} M to 1×10^{-9} M, and the second section corresponds to solutions with C-107 content from 1×10^{-8} M to 1×10^{-4} M. Both plots include several orders of magnitude values of the calix[4]arene content. The PL quenching in individual intervals is insignificant, despite a strong change in the content of C-107. This behavior of the PL quenching is unusual for many molecular systems, primarily, BSA proteins, HSA and drugs [17–21]. It can be assumed that the known PL quenching mechanisms described by the Stern–Volmer equation or its modifications cannot be used for this system. The PL quenching is observed, but its more complex behavior is caused by the complex nature of the intermolecular interaction due to different binding forces, that are possible for the considered molecules. It is important that the quenching

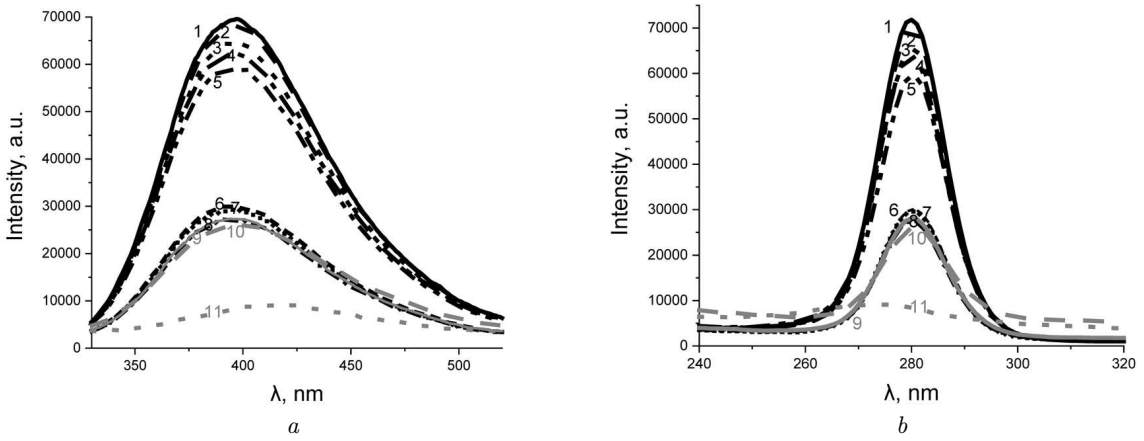

Fig. 4. Spectra of emission (*a*) and excitation (*b*) PL for aqueous solutions of ATP–C-107 (for C-107 DMSO 5%) with a constant concentration of ATP $C_{ATP} = 1 \times 10^{-4}$ M and concentrations of the calix[4]arene $C_{C\text{-}107}0$ (solid line *1*), 1×10^{-12} M (dashed line *2*), 1×10^{-11} M (dotted line *3*), 1×10^{-10} M (dashed-dotted line *4*), 1×10^{-9} M (dashed-double dotted line *5*), 1×10^{-8} M (short dashed *6*), 1×10^{-7} M (short dotted *7*), 1×10^{-6} M (short dashed-dotted *8*), 1×10^{-5} M (grey solid line *9*), 1×10^{-4} M (grey dashed line *10*), and also for a solution in water C-107 with DMSO (5%) at $C_{C\text{-}107} = 1 \times 10^{-4}$ M (grey dotted line *11*) (for ATP–C-107 (*1–10*) $\lambda_{ex} = 282$ nm, $\lambda_{em} = 395$ nm, for C-107 (*11*) $\lambda_{ex} = 275$ nm, $\lambda_{em} = 415$ nm (pH 6.5, $T = 21$ °C))

of the PL is not proportional to the ligand (receptor) concentration. But, at some sets of the concentrations, the dependence on the level of ligands takes place. At the same time, interaction in the complexes is not intensive for both concentration ranges, despite the different binding mechanisms.

It should be noted that the similar PL quenching behavior for the ATP–C-107 system is observed for the excitation with $\lambda_{ex} = 272$ nm, Fig. 5.

The excitation at $\lambda_{ex} = 272$ nm, which corresponds to the absorption band of C-107 does not change the position of the ATP emission band near $\lambda_{em} = 395$ nm. The insignificant PL quenching is observed at low concentrations of C-107 up to 1×10^{-10} M. The quenching increases sharply at the next concentration of 1×10^{-9} M, and, at a concentration of 1×10^{-8} M, a jump in the PL quenching is observed. For higher concentrations of C-107, the PL quenching becomes negligible again. The total PL intensity for ATP–C-107 mixtures decreases significantly.

The PL quenching becomes more difficult for higher concentrations of C-107 in the range from 1×10^{-4} M to 10×10^{-4} M at $\lambda_{ex} = 275$ nm. In this range of concentrations, after a sharp drop in the PL emission intensity for the ATP mixture with the content of C-107 $C_{C\text{-}107} = 1 \times 10^{-4}$ M in relation to the intensity of the band of ATP with $C_{ATP} = 3 \times 10^{-4}$ M, a slight quenching is observed. At the same time, with an increase in the C-107 content, the PL band shifts from 395 nm to 415 nm, that is, the position of the PL maximum for calix[4]arene C-107.

It is known that ATP forms not only supramolecular complexes, which is accompanied by the effect on hydrolysis processes, but also complexes with metals, in which the binding parameters of terminal anhydride bonds are also modulated.

Figure 6 shows the nature of the PL quenching of ATP molecules in water solutions with increasing the $AgNO_3$ concentration from 1×10^{-4} M to 10×10^{-4} M in the presence of calix[4]arenes C-107. For all solutions, the content of C-107 remains constant (1×10^{-4} M).

It can be seen that the addition of C-107 molecules (1×10^{-4} M) to the water solution of ATP leads to a decrease in the PL intensity by two times. Further titration of the aqueous solution of ATP–C-107 with silver ions Ag^+ (1×10^{-4} M) results in the further PL quenching, which changes slightly with an increase in the metal content up to 1×10^{-3} M.

It is worth noting that in the absence of Ag^+ ions in the solutions at the same C-107 concentrations, with an increase in the calix[4]arene content, there is a shift of the PL band to its position for C-107 solutions with increasing the intensity. In the presence of Ag^+, the rearrangement of the specified PL band does not occur during the PL quench-

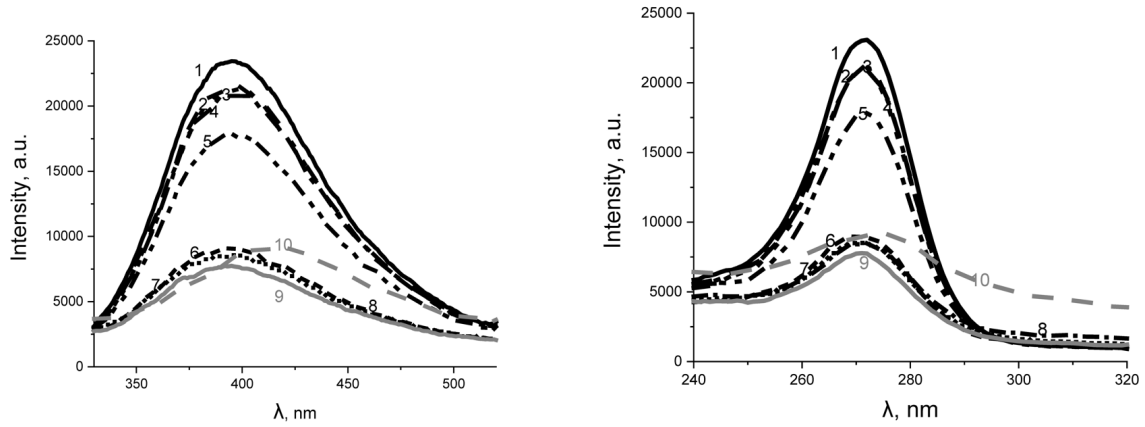

Fig. 5. Emission (*a*) and excitation (*b*) PL spectra for water solutions of ATP–C-107 with a constant concentration of ATP $C_{ATP} = 1 \times 10^{-5}$ M and the content of calix[4]arene (DMSO content is 5%) C-07 0 (solid line *1*), 1×10^{-12} M (dashed line *2*), 1×10^{-11} M (dotted line *3*), 1×10^{-10} M (dashed-dotted line *4*), 1×10^{-9} M (dashed-double dotted line *5*), 1×10^{-8} M (short dashed *6*), 1×10^{-7} M (short dotted *7*), 1×10^{-6} M (short dashed-dotted *8*), 1×10^{-5} M (grey solid line *9*), at $\lambda_{ex} = 282$ nm, $\lambda_{em} = 395$ nm, as well as for a solution of C-107 in water (DMSO content 5%) with a concentration of $C_{C\text{-}107} = 1 \times 10^{-4}$ M at $\lambda_{ex} = 275$ nm, $\lambda_{em} = 415$ nm (grey dashed line (*10*)), (pH 6.5, $T = 21$ °C)

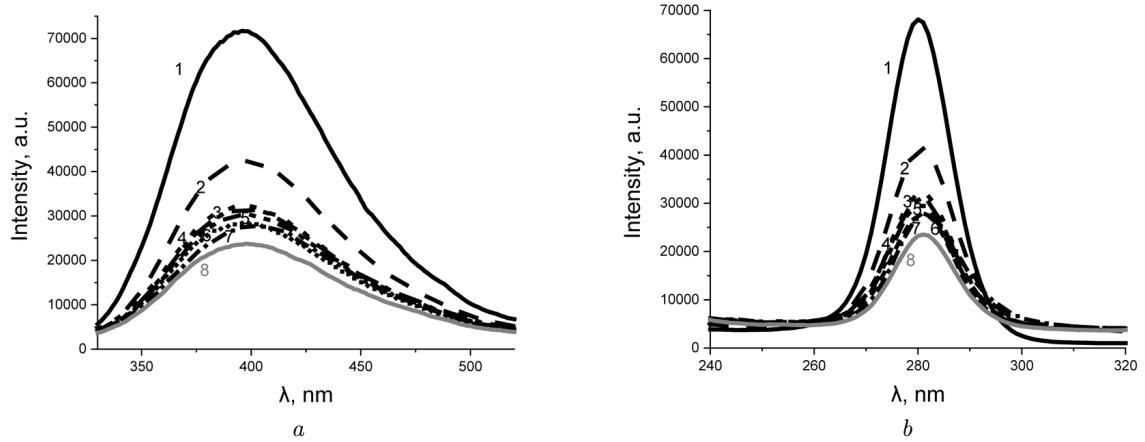

Fig. 6. Emission (*a*) and excitation (*c*) spectra of PL for water solutions of ATP at constant concentrations of $C_{ATP} = 1 \times 10^{-4}$ M (solid line *1*) ATP–C-107 at a constant concentration of $C_{C\text{-}107} = C_{ATP} = 1 \times 10^{-4}$ M (dashed line *2*), ATP–C-107–$AgNO_3$ with concentrations $C_{Ag^+} = 1 \times 10^{-4}$ M (dotted line *3*), 2×10^{-4} M (dashed-dotted line *4*), 4×10^{-4} M (dashed-double dotted line *5*), 6×10^{-4} M (short dashed *6*), 8×10^{-4} M (dashed-double dotted line *7*), 1×10^{-3} M (grey solid line *8*) ($\lambda_{ex} = 280$ nm, $\lambda_{em} = 395$ nm, pH 5.8, $T = 20$ °C)

ing, which indicates the stabilization of ATP–C-107 complexes in the presence of Ag^+ ions.

3.3. Computer modeling of complex formation between ATP and C-107

3.3.1. Molecular dynamics

In order to obtain a rough estimate of the possible configurations of the complexes of calix[4]arene and ATP molecules and their binding energy, stability in an aqueous solvents, we applied methods of molecular docking and dynamics. In the framework of modeling, only weak forces of interaction of molecules in complexes being taken into account: electrostatic, van der Waals, hydrogen bonds, and hydrophobic interaction. The simulation was carried out in the AutoDock 4.2.6 software packages with the semi-empirical scor-

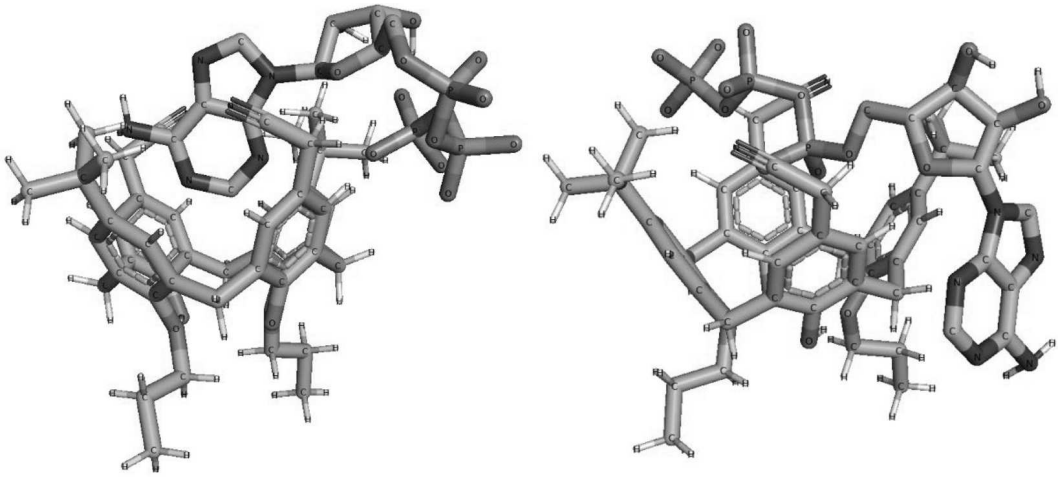

Fig. 7. Configurations of the relative arrangement of calix[4]arene and ATP molecules in the complex: adenine core in the "cup" of calix[4]arene (*a*); adenine backbone on the side, phosphate "tail" above the calix[4]arene "cup" (*b*); adenine backbone and phosphate groups on the side of the "cup" (*c*). The letters and corresponding colors in the figure indicate the chemical elements of the structure of molecules

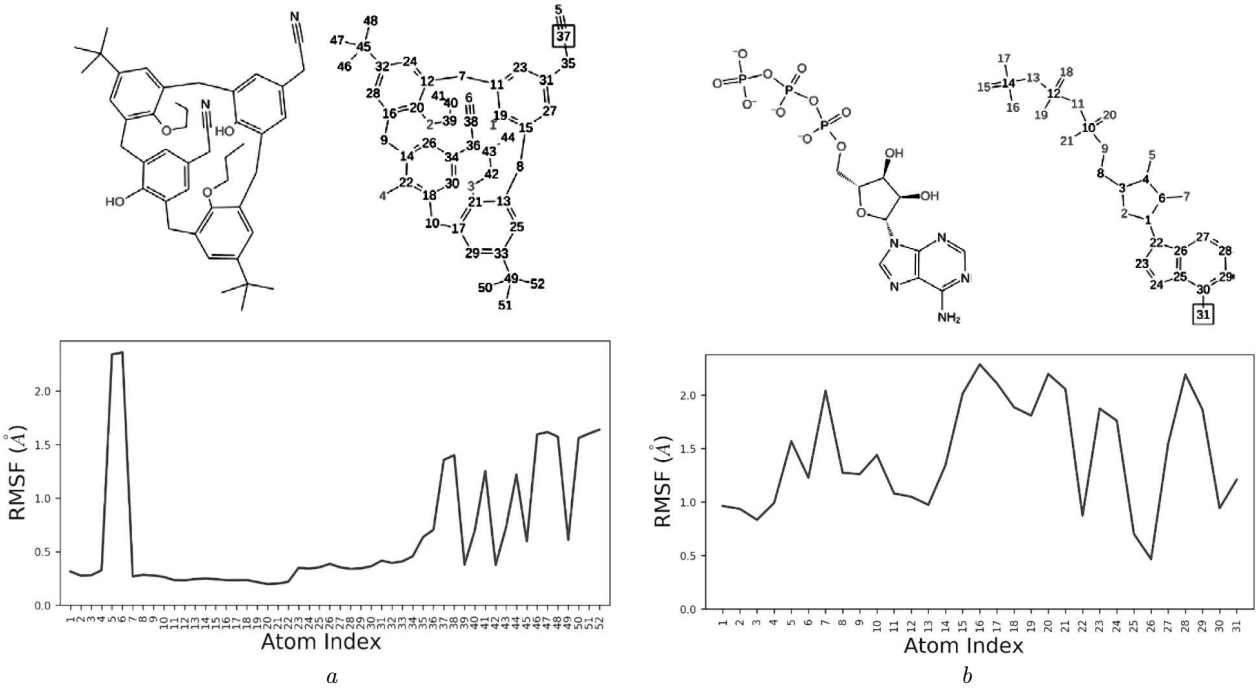

a *b*

Fig. 8. Analysis of deviations of calix[4]arene (*a*) and ATP (*b*) molecules in molecular dynamics

ing function and Lamarckian genetic algorithm for searching the most energetically preferable binding position of ATP-calix[4]arene complex [22, 23].

The molecular docking simulation has determined several possible approximate configurations of the mentioned molecular complexes. The complexes with minimal potential energy are shown in Fig. 7. The binding energy in the complexes presented in the figure $\Delta E_{\text{bind}} \approx -10$ kj/mol (*a*); -9.93 kj/mol (*b*); -8.42 kj/mol (*c*).

The molecular dynamics simulation was performed in Desmond software with OPLSe force field [22] for

the Fig. 7, *a* complex configuration as a starting position in an aqueous solvent. The TIP3P [24] model for water molecules was used. In general, the simulated system contained 3865 atoms without ions in a box of 10 A × 10 A × 10 A size with periodical boundary conditions. The simulation protocol includes the following stages: stage *1* – task; stage *2* – simulation (Brownian Dynamics NVT, $T = 10$ K, small timesteps, and restraints on solute heavy atoms, 100 ps); stage *3* – simulate, NVT, $T = 10$ K, small timesteps, and restraints on solute heavy atoms, 12 ps; stage *4* – simulate, NPT, $T = 10$ K, and restraints on solute heavy atoms, 12 ps; stage *5* – solvate pocket; stage *6* – simulate, NPT and restraints on solute heavy atoms, 12ps; stage *7* – simulate, NPT and no restraints, 24 ps; stage *8* – simulate. In the simulation the stage *5* was skipped by default, which is justified due to the irrelevance of water bridges in the target-ligand complexes formation. NVT and NPT ensembles are taken for Nosé–Hoover thermostat. The last stage is the very simulation of the dynamics for 3 ns with 2 fs time step under normal conditions $T = 300$ K and $p = 1.01325$ bar.

The complex turned out to be stable (Fig. 8), with slight deviations of RMSF=1–2 A for all atoms of the interacting molecules. The Root Mean Square Fluctuation (RMSF) is useful for characterizing changes in the molecule atom positions. The RMSF for atom i is:

$$\mathrm{RMSF}_i = \sqrt{\frac{1}{T}\sum \left(r_i\left(t\right) - r_i\left(t_{\mathrm{ref}}\right)\right)^2},$$

where T is the trajectory time over which the RMSF is calculated, t_{ref} is the reference time (usually for the first frame, and is regarded as the zero of time); r is the position of atom i in the reference at time t_{ref}, and r is the position of atom i at time t after superposition on the reference frame. RMSF may give insights on how ligand fragments interact with the target molecule and their entropic role in the binding event. It gives information about which atoms are the most involved in the interaction, the very magnitude of RMSF describes the mobility of different atoms and the stability of the complex. In particular, the side part of the calix[4]arene "bowl" represented by four carbon rings and the adenine group of the ATP molecule are the least mobile. The most mobile is the phosphate "tail" of ATP and the $-NH_3$ groups of calix[4]arene.

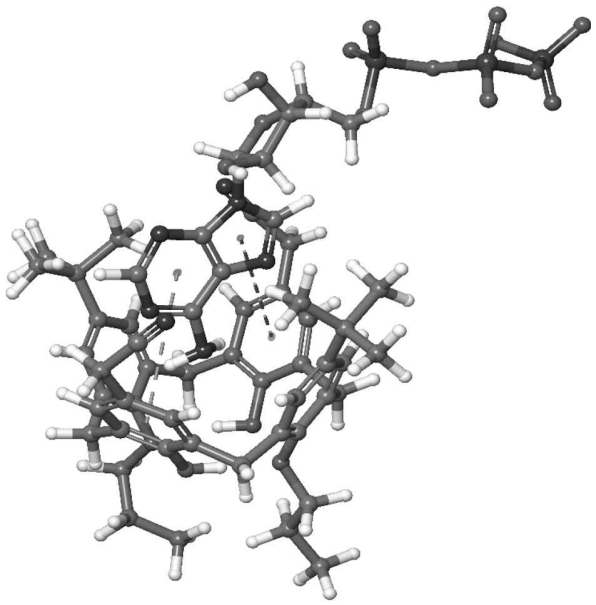

Fig. 9. A molecular complex with an adenine backbone in a calix[4]arene "cup" and a dotted π-π-stacking interaction. The colors correspond to chemical elements similar to Fig. 7

The main complex-forming force is the π-π-stack interaction (Fig. 9) as one of the types of hydrophobic interaction. The interaction occurs between the rings of the adenine group of the ATP molecule and the four carbon rings of calix[4]arene (the intensity of interaction with certain rings changes during the simulation).

3.3.2. Quantum-chemical modeling

The formation of complexes of ATP molecules with calix[4]arene s is also confirmed by quantum-chemical calculations using the density functional method, DFT (B 3 LYP, 3-21 G) Gaussian 03 [25]. The complexes of an ATP molecule with calix[4]arene have been optimized in the following positions of ATP: above the larger diameter of calix[4]arene and near its wall. Changes in the region of the energy gap were detected for the complexes compared to the values of electronic levels for individual components. Thus, the location of the ATP molecule above calix[4]arene leads to a change in the shape of its HOMO molecular orbital, which is localized on a half of the calix[4]arene wall in the complex compared to the symmetric delocalization along the wall in the independent state. The LUMO orbital is localized on both parts of the complex: ATP and top of the calix[4]arene.

In the case of location of ATP along walls of the calix[4]arene, the complexation occurs due to π-π-stacking interaction between parallel arranged the indole fragment of ATP and the phenolic ring of calix[4]arene. The HOMO level of this complex is located on the calix[4]arene, while the LUMO is located on the indole and the calix[4]arene wall. This LUMO orbital, similar to the case of the ATP localization over calix[4]arene, remains unshifted energetically compared to the LUMO levels of individual components, which have almost the same values. However, the HOMO orbital shifts up in both cases: by 0.5 eV for lateral location and by 0.2 eV, when localized above the larger diameter of the calix[4]arene.

The shrinking of the energy gap in these complexes should be manifested in the absorption spectra by a shift to the red region.

4. Conclusion

For water solutions of ATP and calix[4]arenes C-107 at a constant concentration of ATP molecules with an increase in the content of C-107, a complex nature of the PL quenching is observed, while maintaining the position of the PL band near 395 nm (λ_{ex} = 285 nm). Its complexity is based, on the one hand, in the wide range of concentrations of C-107, at which it occurs, and, on the other hand, there are gaps in the quenching values for individual concentrations of calix[4]arene, near which it changes slightly. The indicated nature of PL quenching significantly depends on the value of λ_{ex}, as well as the temperature. A similar quenching behavior is preserved, when $AgNO_3$ salts are added to the ATP–C-107 mixtures, ($C_{ATP} = C_{C\text{-}107} = 1 \times 10^{-4}$ M) in the concentration range from 1×10^{-4} M to 1×10^{-3} M. An increase in the content of Ag^+ ions, which, in turn, forms complexes with the ATP, leads to an increase in the PL quenching, which remains insignificant. At the same time, in the presence of Ag^+ ions, there is no shift of the band near 395 nm toward the position of the band for C-107 (415 nm). Computer modeling shows that the system ATP–C-107 can form energetically stable complexes, when ATP is located on the top of the calix[4]arene and along the wall of it due to π-π-stacking interaction and the complexes are characterized by d shrinking of the energy bands.

The authors sincerely express their gratitude to Kosterin Sergiy Oleksiyovych, Palladin Institute of Biochemistry, National Academy of Sciences of Ukraine and Kalchenko Vitaly Ivanovych, Rodik Roman Vasyliovych Institute of Organic Chemistry, National Academy of Sciences of Ukraine, for their invaluable scientific support throughout the duration of this research.

1. A.H. Pakiaria, M. Farrokhnia, A. Moradshahi. Quantum chemical analysis of ATP, GTP and related compounds in gas phase. *Chem. Soc.* **7**, 51 (2010).
2. F. Meurer, H.T Do, G. Sadowski, C. Held. Standard Gibbs energy of metabolic reactions: II. Glucose-6-phosphatase reaction and ATP hydrolysis. *Biophys. Chem. A* **223**, 30 (2017).
3. J. Dunn, M.H Grider. Physiology, adenosine triphosphate. In: *StatPearls. Treasure Island (FL)* (StatPearls Publishing, 2021).
4. C.H Lee, H.C. Huang, H.F Juan. Reviewing ligand-based rational drug design: The search for an ATP synthase inhibitor. *Intern. J. Mol. Sci.* **12** (8), 5304 (2011),
5. R. Jastrzab, Z. Hnatejko, T. Runka, A. Odanic, L. Lomozika. Stability and mode of coordination complexes formed in the silver (i)/nucleoside systems. *New J. Chem.* **35**, 1672 (2011).
6. F.T. Patrice, L. Zhao, E.K. Fodjo, D.Li, Y. Long. Spectroelectrochemical study of the AMP–Ag^+ and ATP–Ag^+ complexes using silver mesh electrodes. *Analyst.* **143**, 2342 (2018).
7. S. Santi, A.W. Wahab, I. Raya, A. Ahmad, M. Maming. Synthesis, spectroscopic (FT-IR, UV–visible) study, and HOMO-LUMO analysis of adenosine triphosphate (ATP) doped trivalent terbium. *J. Mol ecular Structure* **1237**, 130398 (2021).
8. V.G. Pivovarenko, O.B. Vadzyuk, S.O. Kosterin. Fluorometric detection of adenosine triphosphate with 3-hydroxy-4'-(dimethylamino) flavone in aqueous solutions. *J. Fluorescence* **16**, 9 (2006).
9. V.G. Pivovarenko, O. Bugera, N. Humbert, A.S. Klymchenko, Y. Mély. A toolbox of chromones and quinolones for measuring a wide range of ATP concentrations. *Chem. Eur. J.* **23**, 11927 (2017).
10. D.A. Yushchenko, M.D. Bilokin, O.V. Pyvovarenko, G. Duportail, Y. Me'lyb, V.G. Pivovarenko. Synthesis and fluorescence properties of 2-aryl-3-hydroxyquinolones, a new class of dyes displaying dual fluorescence. *Tetrahedron Lett.* **47**, 905 (2006).
11. L. Liu, L. Zhao, D. Cheng, X. Yao, Y.L. Highly. Highly selective fluorescence sensing and imaging of ATP using a boronic acid groups-bearing polythiophene derivate. *Polymers* **11**, 1139 (2019).
12. S.O. Kosterin, V.I. Kalchenko, T.O. Veklich *et al. Calixarenes as Modulators of ATP-Hydrilizing Systems of Smooth Muscles* (Scientific Opinion, 2019), **15**, 2.
13. T.O. Veklich, S.O. Kosterin, R.V. Rodik *et al.* Effect of calixarene-phosphonic acid on Na+, K+-ATPase activ-

ity in plasma membranes of the smooth-muscle cells *Ukr. Biochem. J.* **78**, 70 (2006).
14. Y. Tian-Ming, Y. Zhi-Feng, W. Li, G. Jin-Ying, Y. Si-De, S. Xian-Fa. Supramolecular interaction between water-soluble cali[4]xarene and ATP–the catalysis of calix[4]arene for hydrolysis of ATP. *Spectrochimica Acta Part* **58** (14), 3033 (2002).
15. A.V. Lohvyn. O.P. Dmytrenko, M.P. Kulish, O.L. Pavlenko, A.P. Naumenko, A.I. Lesiuk, T.O. Veklich, M.I. Kaniuk. Spectral features of adenosine triphosphate solutions with calix[4]arene C-107. *Appl. Nanosci.* **13**, 4809 (2023).
16. N.A. Goncharenko, O.L. Pavenko, O.P. Dmytrenko. Complexation in aqueous solutions of doxorubicin, bovine serum albumin and gold nanoparticles. *Appl. Nanosci. A* **10** (8), 2941 (2020).
17. N.A. Goncharenko, O.L. Pavenko, M.P. Kulish *et al.* Gold nanoparticles as a factor of influence on doxorubicin–bovine serum albumin complex. *Appl. Nanosci. A* **9** (5), 825 (2019).
18. L.A. Bulavin *et al.* Heteroassociation of antitumor agent doxorubicin with bovine serum albumin in the presence of gold nanoparticles. *J. Mol. Liq. A* **284**, 633 (2019).
19. N.A. Goncharenko, O.P. Dmytrenko, M.P. Kulish *et al.* Mechanisms of the interaction of bovine serum albumin with anticancer drug gemcitabine. *Mol. Cryst. Liq. Cryst. A* **701** (1), 59 (2020).
20. O. Dmytrenko, M. Kulish, O. Pavlenko *et al.* Mechanisms of heteroassociation of ceftriaxone and doxorubicin drugs with bovine serum albumin. *Soft Mat. Sys. Biomed. App. A* **226**, 219 (2022).
21. S.F. Sousa, P.A. Fernandes, M.J. Ramos. Protein–ligand docking: Current status and future challenges. *Proteins.* **65** (1), 15 (2006).
22. G.M. Morris., R. Huey, W. Lindstrom *et al.* AutoDock4 and AutoDockTools4: Automated docking with selective receptor flexibility. *J. Comput. Chem. Dec* **30** (16), 2785 (2009).
23. K. Roos, C. Wu, W. Damm *et al.* OPLS3e: Extending force field coverage for drug-like small molecules *J. Chem. Theory and Computatio* **15** (3), 1863 (2019).
24. W.L. Jorgensen, J. Chandrasekhar, J.D. Madura *et al.* Comparison of simple potential functions for simulating liquid water. *J. Chem. Phys.* **79** (2), 926 (1983).
25. M.J. Frisch, G.W. Trucks, H.B. Schlegel, G.E. Scuseria, M.A. Rob, J.R. Cheeseman, J.A. Montgomery Jr., T. Vreven, K.N. Kudin, J.C. Burant, J.M. Millam, S.S. Iyengar, J. Tomasi, V. Barone, B. Mennucci, M. Cossi, G. Scalmani, N. Rega, G.A. Petersson, H. Nakatsuji, M. Hada, M. Ehara, K. Toyota, R. Fukuda, J. Hasegawa, M. Ishida, T. Nakajima, Y. Honda, O. Kitao, H. Nakai, M. Klene, X. Li, J.E. Knox, H.P. Hratchian, J.B. Cross, V. Bakken, C. Adamo, J. Jaramillo, R. Gomperts, R.E. Stratmann, O. Yazyev, A.J. Austin, R. Cammi, C. Pomelli, J.W. Ochterski, P.Y. Ayala, K. Morokuma, G.A. Voth, P. Salvador, J.J. Dannenberg, V.G. Zakrzewski, S. Dapprich, A.D. Daniels, M.C. Strain, O. Farkas, D.K. Malick, A.D. Rabuck, K. Raghavachari, J.B. Foresman, J.V. Ortiz, Q. Cui, A.G. Baboul, S. Clifford, J. Cioslowski, B.B. Stefanov, G. Liu, A. Liashenko, P. Piskorz, I. Komaromi, R.L. Martin, D.J. Fox, T. Keith, M.A. Al-Laham, C.Y. Peng, A. Nanayakkara, M. Challacombe, P.M.W. Gill, B. Johnson, W. Chen, M.W. Wong, C. Gonzalez, J.A. Pople. *Gaussian 03* (Gaussian, Inc., Wallingford, CT, 2003).

Received 09.11.23

А. Стражинська, О. Дмитренко,
М. Куліш, О. Павленко, І. Дорошенко,
А. Лесюк, Т. Векліч, М. Канюк

ОСОБЛИВОСТІ ГАСІННЯ
ФЛУОРЕСЦЕНЦІЇ В РОЗЧИНАХ
У ВОДІ АТФ – КАЛІКС[4]АРЕНА С-107

Досліджувався характер гасіння флуоресценції (ФЛ) для розчинів у воді АТФ–С-107 і АТФ–С-107–$AgNO_3$. Для розчинів у воді АТФ–С-107 при збереженні вмісту ($1 \cdot 10^{-4}$ М або $3 \cdot 10^{-4}$ М) та підвищенні концентрації С-107 спостерігається складний характер гасіння ФЛ. В першу чергу, помітне гасіння ФЛ відбувається в широкому інтервалі концентрацій від $1 \cdot 10^{-12}$ М до $1 \cdot 10^{-4}$ М, що утруднює застосування рівнянь Штерна–Фольмера для визначення констант гасіння і зв'язування. З іншого боку, мають місце розриви в гасінні ФЛ для деяких концентрацій С-107, поблизу яких гасіння незначне. Поведінка гасіння ФЛ змінюється від величини λ_{ex} і температури при збереженні положення смуги ФЛ для АТФ (395 нм). Подібний характер гасіння ФЛ зберігається при додаванні до розчинів АТФ–С-107 солі $AgNO_3$. При сталих значеннях $C_{АТФ} = C_{С\text{-}107} = 1 \cdot 10^{-4}$ М збільшення вмісту Ag^+ приводить до незначного гасіння ФЛ, яке свідчить про утворення комплексів АТФ–Ag^+. Комп'ютерне моделювання для вказаних систем вказує на формування в розчинах у воді комплексів АТФ–С-107 і АТФ–С-107–Ag^+, поява яких супроводжується зміною конформацій АТФ, електронної структури, що знаходить підтвердження в коливальних спектрах ІЧ-поглинання.

Ключові слова: аденозитрифосфат, калікс[4]арен С-107, гасіння флуоресценції, комп'ютерне моделювання, ІЧ-поглинання.